RL-TR-94-43
In-House Report
March 1994

MEASUREMENTS OF HF AURORAL CLUTTER USING THE VERONA AVA LINEAR ARRAY RADAR (VALAR)

David S. Choi, Bertus Weijers, and Neil B. Myers

APPROVED FOR PUBLIC RELEASE; DISTRIBUTION UNLIMITED.

Rome Laboratory
Air Force Materiel Command
Griffiss Air Force Base, New York

This report has been reviewed by the Rome Laboratory Public Affairs Office (PA) and is releasable to the National Technical Information Service (NTIS). At NTIS it will be releasable to the general public, including foreign nations.

RL-TR-94-43 has been reviewed and is approved for publication.

APPROVED: Robert V. McGahan

ROBERT V. McGAHAN
Chief, Applied Electromagnetics Division
Electromagnetics & Reliability Directorate

FOR THE COMMANDER: John K. Schindler

JOHN K. SCHINDLER
Director of Electromagnetics & Reliability

If your address has changed or if you wish to be removed from the Rome Laboratory mailing list, or if the addressee is no longer employed by your organization, please notify RL (ERCP) Hanscom AFB MA 01731. This will assist us in maintaining a current mailing list.

Do not return copies of this report unless contractual obligations or notices on a specific document require that it be returned.

REPORT DOCUMENTATION PAGE

Form Approved
OMB No. 0704-0188

1. AGENCY USE ONLY (Leave blank)	2. REPORT DATE	3. REPORT TYPE AND DATES COVERED
	March 1994	In-house, June 90-June 91

4. TITLE AND SUBTITLE
Measurements of HF Auroral Clutter Using the Verona Ava Linear Array Radar (VALAR)

5. FUNDING NUMBERS
PE: 62702F
PROJ NO: 4600
TASK NO: 460016
WORK UNIT: 46001610

6. AUTHOR(S)
David S. Choi
Bertus Weijers
Neil B. Myers

7. PERFORMING ORGANIZATION NAME(S) AND ADDRESS(ES)
Rome Laboratory/ERCP
31 Grenier Street
Hanscom AFB, MA 01731-3010

8. PERFORMING ORGANIZATION REPORT NUMBER
RL-TR-94-43

9. SPONSORING/MONITORING AGENCY NAME(S) AND ADDRESS(ES)

10. SPONSORING/MONITORING AGENCY REPORT NUMBER

11. SUPPLEMENTARY NOTES

12a. DISTRIBUTION/AVAILABILITY STATEMENT
Approved for Public Release; Distribution Unlimited

12b. DISTRIBUTION CODE

13. ABSTRACT (Maximum 200 words)
Measurements of high frequency (HF) auroral clutter using the Verona Ava Linear Array Radar (VALAR) system are presented. VALAR is an experimental HF backscatter system capable of obtaining high resolution synoptic mapping of HF auroral clutter. The receive system includes a 700 meter long linear array, providing the high azimuthal resolution required for determiming the spatial distribution of HF auroral clutter. Since the completion of the system at the end of 1989, data acquisition campaigns have been carried out on a near-monthly basis. In this report, we provide a brief description of VALAR and present preliminary measurements of three types of phenomena: ground backscatter, slant-F, and auroral backscatter.

14. SUBJECT TERMS
HF auroral clutter, OTH-B radar clutter,
High-latitude backscattered signals

15. NUMBER OF PAGES
26

16. PRICE CODE

17. SECURITY CLASSIFICATION OF REPORT	18. SECURITY CLASSIFICATION OF THIS PAGE	19. SECURITY CLASSIFICATION OF ABSTRACT	20. LIMITATION OF ABSTRACT
Unclassified	Unclassified	Unclassified	SAR

Contents

Illustrations

Measurements of HF Auroral Clutter Using the Verona Ava Linear Array Radar (VALAR)

1. INTRODUCTION

Over-the-horizon backscatter (OTH-B) radar systems operate in the high frequency (HF) band from 6 to 30 MHz. These systems are used to detect and track targets at distances beyond the line-of-sight range, typically from 500 to 3000 km. Detection and tracking at long ranges is possible because the signals in this frequency band can propagate to the ground beyond the line-of-sight distance of the transmitter via oblique reflection from the ionosphere. The backscattered signal from the ground is returned to the receive array, generally located within 100 to 200 km from the transmitter, by a second oblique reflection from the ionosphere. If there are moving targets within the illuminated region, the backscattered signals from the targets are also returned to the receive array via similar ionospheric ray paths. The radar processing of the received signals then allows the detection and tracking of these targets.

OTH-B radar systems operating at high latitudes, however, are subject to periods of degradation in performance due to the presence of magnetic field-aligned electron density irregularities in the high latitude ionosphere. When the propagation vector of the HF signal is perpendicular (or almost perpendicular) to these field-aligned irregularities, the backscattered signal can return to the receive

(Received for Publication 11 March 1994)

array and interfere with detection and tracking of the desired targets. The HF signal propagating in this region can be backscattered to the receive array due to scattering from (1) small-scale F-region irregularities, (2) irregularities located in the sub-auroral region, and (3) large-scale irregularities in the auroral ionosphere.[1] These irregularities can be envisioned as randomly distributed cylindrical blobs or patches elongated in the direction of the Earth's magnetic field lines. In the high latitude ionosphere near the auroral zone, these irregularities tend to drift with a distribution of velocities in the general direction of the ionospheric plasma in which they are embedded, causing both Doppler shifts and spreads in the backscattered signal. This unwanted backscattered radar signal is termed auroral clutter and is one of the identified sources of residual clutter encountered by OTH-B radars operating near or at high latitudes. Many important properties of auroral clutter remain unidentified, requiring extensive analysis and characterization prior to the development and evaluation of clutter mitigating techniques.

In recognition of the need to address HF residual clutter issues that are critical to HF surveillance technology, Rome Laboratory developed an experimental backscatter radar system, the Verona-Ava Linear Array Radar (VALAR). The primary mission of VALAR is to investigate the characteristics of HF residual clutter and to explore and develop modern digital signal processing techniques that could lead to an improvement in the performance of current and future HF radar systems. The system consists of a 700-meter receive antenna array and 36 identical HF receivers controlled by a MicroVAX II computer. Since its completion at the end of 1989, various in-house, short-term experiments have been performed. This report presents some preliminary results from an on-going HF auroral clutter mapping experiment. A brief system description will be presented followed by some initial results from measurements of HF auroral clutter obtained during 1990.

2. VALAR SYSTEM DESCRIPTION

The VALAR system is geographically located at 43.1° N, 75.3° W. VALAR was designed to carry out various experiments to investigate HF radar clutter issues and to develop digital signal processing techniques applicable to OTH-B radar systems. The radar location and its coverage area are shown in Figure 1. The coverage area extends in azimuth from 20° west to 40° east of geographic north and in slant range from 500 to 2500 km. The 13 beams indicated in the figure are the azimuth beams formed prior to the range-Doppler processing. These 13 beams are steered at 5° increments over the 60° coverage area of VALAR. For example, beams 1, 7, and 9 are 20° west, 10° east, and 20° east of geographic north, respectively. Also depicted in Figure 1 is the approximate position of the auroral oval at 2100 hr local time (LT) for a typical magnetic index of Q=3.[2] It is clear from the figure that

---

[1] Moller, H.G. (1984), Backscatter results from Lindau. II. The movement of curtains of intense irregularities in the polar F layer, *J. Atmos. Terr. Phys.*, 36:1487-1501.

[2] Whalen, J. A. (1970), *Auroral Plotter and Nomograph for Determining Corrected Geomagnetic Local Time, Latitude for High Latitudes in the Northern Hemispheres*, AFCRL-70-0422, AD 713170.

both the equatorward and poleward boundaries of the auroral oval are within the field of view of VALAR.

2.1 Transmit System

The transmit system of VALAR is located at the Rome Laboratory RF facility at Ava, New York. The Ava facility includes various antennas and transmitters and is capable of providing desired transmit radiation characteristics for HF signals in the 2 to 30 MHz band at up to 300 kW rms power. Near-total azimuth coverage is possible by selecting one of various HF antennas in different configurations. For the spread clutter data acquisition campaigns, a rhombic antenna was used because it supported the low launch angle and high transmit power requirements of OTH-B experiments. At 10 MHz, the theoretical 3 dB elevation beamwidth of this rhombic is 14° centered at 10° elevation. The theoretical 3 dB azimuthal beamwidth is also 14°.

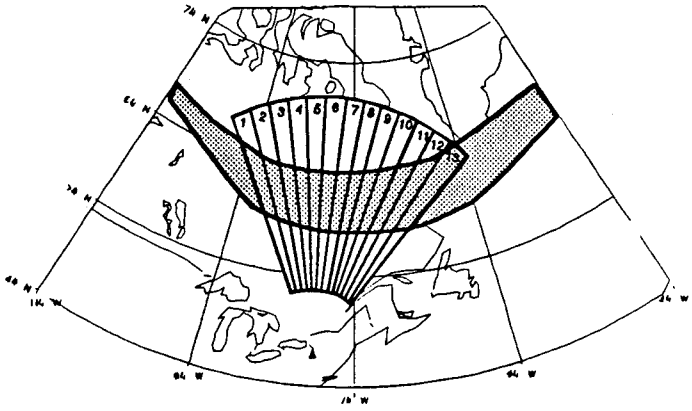

Figure 1. Expected Position Coverage Area of VALAR and the Auroral Oval at 2100 hr Local Time for Magnetic Index of Q=3.

The Ava facility is capable of providing various transmit waveforms including wideband Swept-Frequency Continuous Wave (SFCW) and narrowband linear Frequency-Modulated Continuous Wave (FMCW) signals. During data acquisition the facility simultaneously transmitted both the SFCW and FMCW waveforms. The wideband SFCW signal was required to provide signals for the oblique sounder receiver located near the VALAR receive array at Verona. The oblique sounder was swept from 4 to 30 MHz and was used to generate backscatter ionograms for determining the propagation conditions during data acquisition. The narrowband FMCW modulated over a 10 kHz bandwidth was the waveform used for all data acquisition.

2.2. Receive System

The receive system is located at the Rome Laboratory Verona Test Annex at Verona, NY. It features a unique elemental data recording capability, which is required for the development and the evaluation of digital signal processing clutter-mitigating techniques. The basic block diagram of VALAR is shown in Figure 2. It consists of 36 receive elements with preamplifiers, 36 identical narrow band HF receivers, a MicroVAX II, and a Kennedy 6470 tape drive. A brief description of the antenna array, system electronics, and data acquisition/processing software will be presented in this section.

2.2.1 RECEIVE ANTENNA ARRAY

The receive antenna array extends 700 meters in length with its boresight at 10° east of geographic north. The configuration of the receive array, shown in Figure 3, consists of 36 subarrays of two active and two passive monopoles with a subarray spacing of 20 meters. The array was designed to optimize the system performance over the frequency band of 6 to 12 MHz because auroral clutter is predominantly a nighttime phenomenon and the ionosphere does not support higher frequencies during this period. Previous antenna pattern measurements at 12 MHz have indicated a 2.5° half-power beamwidth (unweighted), 23 dB array gain, and 30 dB RMS sidelobe levels.[3]

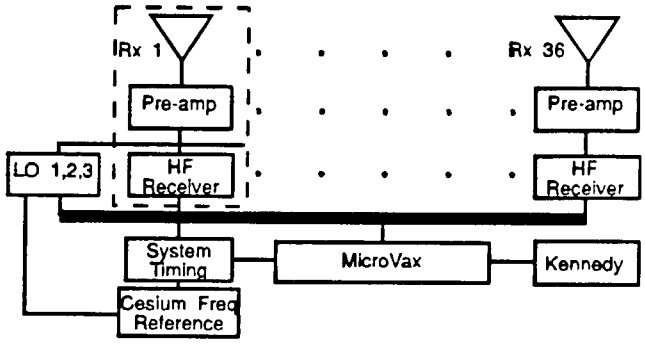

Figure 2. VALAR System Block Diagram, Consisting of 36 Subsystems Containing an Antenna Subarray, a Preamplifier, and an HF Receiver.

2.2.2 RECEIVE SYSTEM ELECTRONICS

The receive system electronics consists of 36 preamplifiers and HF receivers. The HF signal received by the two active monopoles of a subarray are power combined prior to the input of the preamplifier, which filters and amplifies the signal. Each receiver then converts the HF signal at the output of the preamplifier to a complex digital signal as follows. The HF signal is first up-converted to an RF frequency of 42.905 MHz, filtered, and then amplified. This resultant RF signal is down-converted to an IF signal of 10.7 MHz. The IF signal is then power divided for subsequent quadrature demodulation over two independent channels, to obtain the in-phase (I) and quadrature (Q) components of the signal. The resultant I and Q signals are then filtered using a 5 kHz lowpass filter prior to the sample and hold circuitry of the A/D converter. The digitized baseband data sampled at 10 kHz are temporarily buffered in RAM prior to serial transfer to the MicroVAX II and subsequent recording

2.2.3 DATA AQUISITION AND PROCESSING SOFTWARE

The data acquisition process is driven by the data acquisition software implemented in VMS FORTRAN on the MicroVAX II. Various system parameters, such as the operating frequency and coherent integration time, are specified by the use of the data acquisition software. The data

---

[3] Gould, A. J. (1990), *A Thinned High Frequency Linear Antenna Array to Study Ionospheric Structure*, RADC-TR-90-186, Rome Air Development Center, Rome, NY, ADA240764.

acquisition software also includes diagnostic tools. These tools enable an on-line check of both the system performance and the data quality. The operator may simultaneously view the amplitude, phase, and signal-to-noise ratio of all 36 channels, examine the frequency spectrum of a single channel, and plot the azimuthal distribution of the power incident on the antenna array for a given range.

The processing and analysis of the VALAR database are performed off-line at the Rome Laboratory Propagation Branch at Hanscom AFB. The Branch computer facility includes a MicroVAX and a number of 386 PCs. All data processing is performed on the MicroVAX using the data processing programs written in VMS FORTRAN.

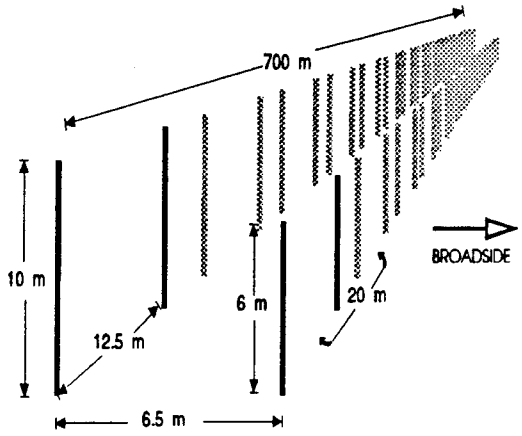

Figure 3. Configuration of VALAR Antenna Array Consisting of 36 Subarrays and Extending 700 Meters in Length. The four elements in darker lines illustrate the geometry of a subarray containing two active and two passive monopoles.

3. HF BACKSCATTER MEASUREMENTS

In this section we present some examples of measurements made using VALAR during two separate data acquisition campaigns. The data acquired on 24 September 1990 will be presented in Section 3.1 to identify and describe the characteristics of various modes of backscattered signals observed using VALAR. These data will be presented in the form of amplitude-range-azimuth (ARA) and amplitude-range-Doppler (ARD) maps. For the ARA maps, the height of the ionosphere was assumed to be 300 km so as to overlay the HF backscatter data on a map with geographic coordinates. A more detailed discussion of the data will be presented in Section 4.

3.1 Characteristics of HF Backscattered Signals

On 24 September 1990, HF backscatter data were collected from 1900 to 2400 hr LT (all times referenced hereafter will be in local time). The Kp index was 3, which indicates moderate geomagnetic activity. Auroral backscatter (See Figure 4(b)) began to appear in the ionograms around 2040 hr. A sequence of snapshots of HF backscatter data were acquired from 2020 to 2250 hr (Figures 5 and 6) using a coherent integration time of 3.2 seconds and an operating frequency of 10.58 MHz. A waveform repetition frequency (WRF) of 25 Hz was selected to remove range ambiguities up to 6000 km, thereby limiting the Doppler bandwidth to +/-12.5 Hz. At 2250 hr the intensity of the auroral backscatter decreased significantly at 10.58 MHz, and therefore the operating frequency was changed to 7.87 MHz.

In this section, we present measurements made during the interval from 2020 to 2250 hr. In Section 3.1.1, the north-look backscatter ionograms obtained at Verona, NY will be examined in detail to identify various types of backscattered signals observed during the evening. In Section 3.1.2, the characteristics of ground backscatter under normal ionospheric conditions will be described to present ideal conditions for detection of targets. The measurements of auroral backscatter made during 2100 to 2250 hr will follow in Sections 3.1.3 and 3.1.4, respectively.

3.1.1 BACKSCATTER IONOGRAMS

The north-look backscatter ionograms obtained at 2030 and 2125 hr are shown in Figure 4. These ionograms display the intensity of the backscatter as a function of the slant range and frequency. The level of the intensity is displayed by the darkness of the traces. Because of the AGC, the amplitudes along the range axis are normalized to the maximum intensity of the backscatter at each frequency and, therefore, estimates of relative intensity from frequency to frequency cannot be made from these ionograms.

Figure 4(a) shows a typical backscatter ionogram obtained for normal propagation conditions during early evening. The returned signals at frequencies between 6.5 and 9.5 MHz are from the first and second vertical incidences. The slant range of the first vertical incidence at 6.5 MHz is about 300 km, which is a typical F-layer height. As expected, the slant range of the second vertical incidence is about twice the first. Beyond 9.5 MHz, the ground backscatter emanates from the second vertical incidence and increases in slant range with increasing frequency. This ground backscatter return indicates a signal that is twice reflected from the F-layer in the course of returning to the receiver via a reciprocal ray path. The increase in slant range with frequency is expected since the oblique angle of reflection increases with frequency. From Figure 4(a), at 10.58 MHz, the frequency used for the VALAR data collection, the leading edge of the ground backscatter is at 800 km.

The backscatter ionogram obtained at 2125 hr is shown in Figure 4(b). The slant range of the leading edge of the ground backscatter at 10.58 MHz is now approximately 1200 km. The increase in slant range from 800 km at 2030 hr to 1200 km at 2125 hr is due to the post-sunset increase in F-layer height, which prevailed during the rest of the night.

In addition to the ground backscatter there are additional backscattered signals indicated as "Slant-F" and "Auroral Backscatter" in the ionogram. The trace that begins near the first vertical incidence and increases in slant range with increasing radar frequency has been described by Bates as the slant-F trace and is produced by the small scale, field-aligned irregularities in the F-region ionosphere.[4] Bates[5] and Elkins[6] also demonstrated that the irregularities that produce the slant-F clutter are the same irregularities that produce the spread-F seen using vertical ionosondes. At 10.58 MHz, the leading edge of the slant-F is at about 500 km. Slant-F echoes can occur both in the sub-

---

[4] Bates, H.F. (1960), Direct HF backscatter from the F region, *J. Geophys. Res.*, **65**:1993-2002.

[5] Bates, H.F. (1971), The aspect sensitivity of spread-F irregularities, *J. Atmos. Terr. Phys.*, **33**:111.

[6] Elkins, T.J. (1980), *A Model for High Frequency Radar Auroral Clutter*, RADC-TR-80-122, Rome Air Development Center, Rome, NY, ADA091049.

auroral and the auroral region. From the location of VALAR, however, they are associated with irregularities in the sub-auroral F-layer.[7]

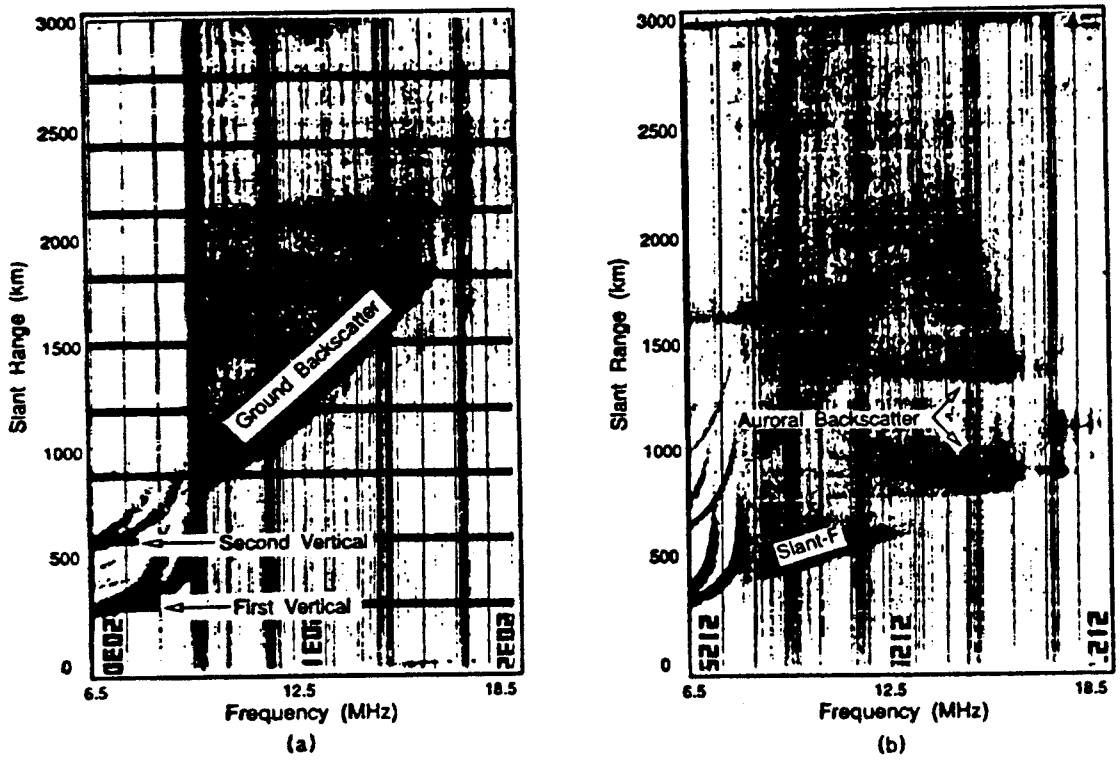

Figure 4. North-Look Backscatter Ionograms Obtained on 24 September 1990 at (a) 2030 hr, Showing the Ground Backscatter Under Normal Propagation Conditions and (b) 2125 hr, Showing Additional Echoes Due to Slant-F and Auroral Backscatter.

The backscattered signals exhibiting constant slant range as a function of radar frequency, and labeled Auroral Backscatter in Figure 4(b), are due to the large-scale irregularities in the high latitude F region ionosphere. These blobs of ionization enhancement have been reported to exist from the lower F region to a height of several hundred kilometers in the high latitude ionosphere.[8] The fact that the signals due to these large-scale irregularities are constant in range is perhaps due to the large electron density gradient of the irregularities. The leading edges of two of these backscattered signals

---

7 Tsunoda, R.L., Basler, R.P., Showen, R.L., Walker, N. P., Frank, V. R., and Lomasney, J. M. (1981), *Investigation of High-Frequency Radar Auroral Clutter and Round-the-World Propagation*, Tech. Rep. 54, 66 pp., SRI Int., Menlo Park, Calif.

8 Vickery, J. F., Rino, C. L., and Potemra, T. A. (1980), Chatanika/TIAD observations of unstable ionization enhancements in the auroral F region, *Geophys. Res. Lett.*, 7:789.

are at 800 and 1300 km slant range, respectively. From a simple geometry relating the expected position of the equatorward boundary of the auroral oval at Q=3 and the location of VALAR, we may conclude that the backscattered signals at 800 km and 1300 km are due to the irregularities in the trough and auroral region F-layer, respectively. The constant range backscatter originating from the auroral zone can appear at both long and short slant ranges. The long slant range is associated with high elevation angles while the short slant range implies low elevation angles.[9]

3.1.2 GROUND BACKSCATTER

Contour plots of the range-azimuth distributions of the backscattered signals at 2030 and 2130 hr are shown in the ARA maps of Figure 5(a) and 5(b), respectively. These contour plots are in 3-dB steps and the relative amplitudes corresponding to the colors are shown in the legend. Ground distances are measured in concentric arcs starting at 500 km and ending at 2500 km in 500 km steps.

The dominant features in Figure 5(a) are the bands of backscattered signals between 800 and 1200 km, which are uniformly distributed in azimuth. In Figure 5(b), these bands are visible between 1200 and 1800 km. Since the range extent of these backscattered signals is in good agreement with the range extent of the ground backscatter seen in the ionograms, they may be identified as ground backscatter.

We can also identify the ground backscatter by analyzing the Doppler distribution of the backscattered signals. The ARD maps obtained at 2030 and 2130 hr are shown in Figure 6(a) and 6(b), respectively. Each row of ARD maps contains 13 map panels displaying the range and Doppler distributions obtained at a given time for the 13 azimuth beams discussed in Section 2. The panels are numbered 1 through 13 starting on the left in the order of increasing clockwise rotation (see Figure 1). For each panel, the x-axis and y-axis correspond to the Doppler and range intervals of -12.5 to 12.5 Hz and 500 to 2500 km, respectively.

Since the ground is a stationary target, it is characterized by a peak Doppler frequency of 0 Hz. Hence ground backscatter can be identified in these ARD maps as backscattered signals with peak Doppler signature at 0 Hz. Figure 6(a) displays the ARD maps obtained at 2030 hr. In these ARD maps the bands of backscattered signals between 800 and 1200 km exhibit 0 Hz peak Doppler frequency, which confirms our conclusion that these signals are ground backscatter. These maps also exhibit some backscattered signals from the ground as far as 2000 km in slant range, indicating the presence of multi-hop modes.

Figure 7 gives a detailed look at the peak Doppler spectra at a slant range of 800 km for beams 3, 5, and 7. These peak Doppler spectra were obtained by finding the range bin with the largest intensity in each beam then averaging over 5 range bins about the range bin with the peak intensity. The ground clutter is approximately 30 dB above the noise floor and the narrow spread is confined to about +/- 1 Hz about 0 Hz, again confirming that these returns are from the ground.

The ARD maps obtained at 2130 hr (Figure 6(b)) show that the bands of backscattered signals between 1200 to 1800 km consist of both ground and auroral backscatter. The ground backscatter is

---

[9] Montbriand, L. E. (1988), Auroral backscatter observed at HF from Ottawa, *Radio Sci*, 23:850-864.

observed in all beams, with highest intensity in beams 1 through 4. It should be noted that the ground backscatter exhibits decreased intensity in range extent in beams 5 through 10, where the slant-F and auroral backscatter are present. This is because some of the transmitted rays were directly backscattered by the field-aligned irregularities and never propagated out to the ground.

(a)

(b)

Figure 5. Amplitude-Range-Azimuth (ARA) Maps Obtained on 24 September 1990, at (a) 2030 LT Showing the Ground Backscatter Starting at 800 km and (b) at 2130 LT Showing the Ground Backscatter Starting at 1200 km with Additional Returns at 500, 800, and 1300 km.

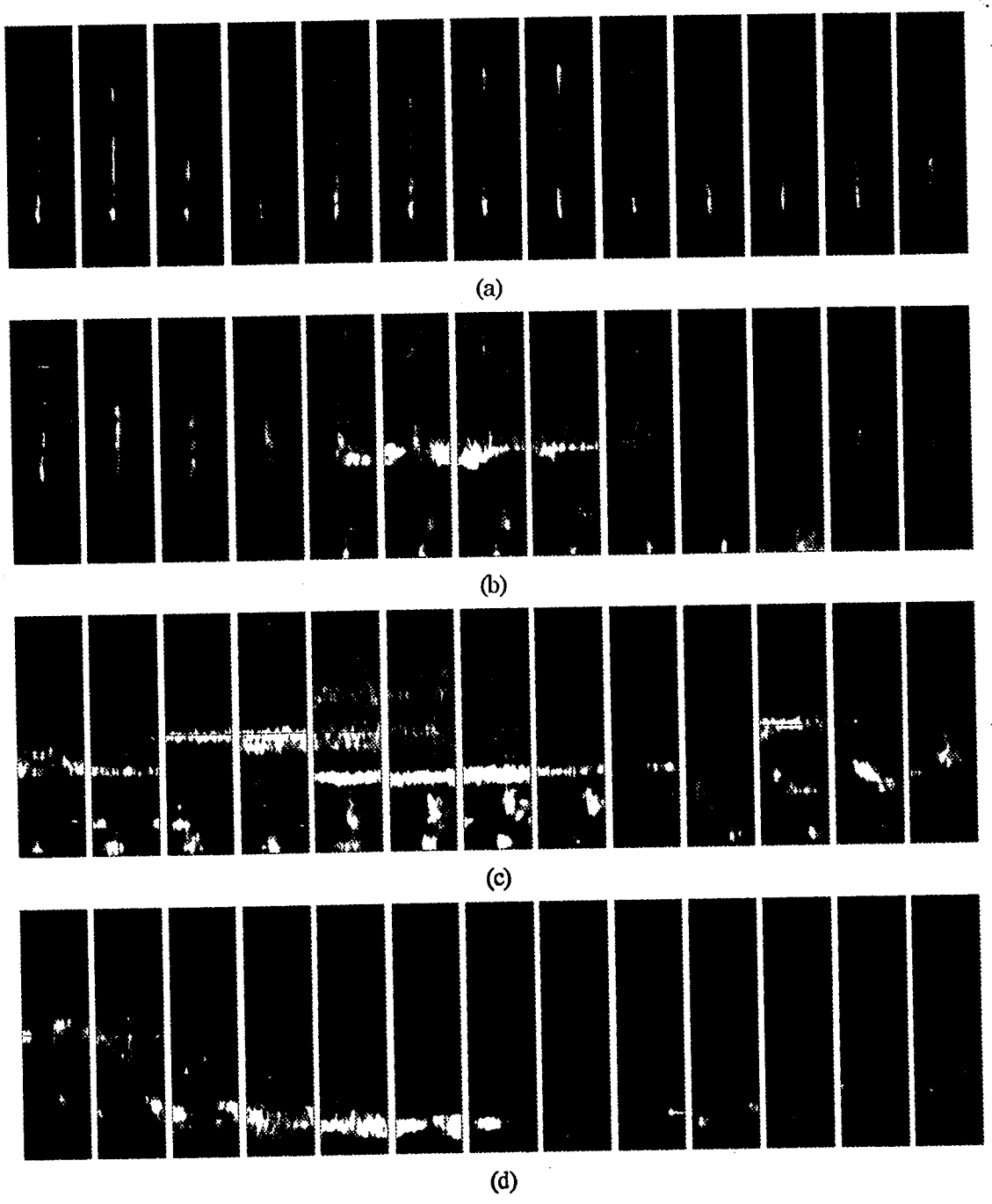

Figure 6. Amplitude-Range-Doppler (ARD) Maps Obtained on 24 September 1990, at (a) 2030, (b) 2130, (c) 2202, and (d) 2242 hr. Part (a) displays the Doppler distribution of ground backscatter while (b)-(d) shows the auroral backscatter at different periods of the night. Each row of ARD maps contains the 13 map panels displaying the range and Doppler distribution at a given time obtained for the 13 azimuth beams discussed in Section 2. For each panel, the x-axis and y-axis correspond to the Doppler and range intervals of -12.5 to 12.5 hz and 500 to 2500 km, respectively.

3.1.3 SLANT-F

Slant-F echoes were described in Section 3.1.1 as directly backscattered signals from small-scale field-aligned irregularities in the sub-auroral F-region ionosphere. It was shown that the leading edge of slant-F occurs at 500 km in the oblique ionograms. The ARA map obtained at 2130 hr (Figure 5(b)) indeed shows backscattered signals between 500 and 600 km slant range. The ARD maps obtained at 2130, 2202, and 2242 hr are presented in Figures 6(b)-6(d). These ARD maps show measurements corresponding to early evening, peak auroral activity period, and late evening, respectively. Slant-F echoes are seen in the ARD maps of Figures 6(b) and 6(c), but they are absent in the measurements made at 2242 hr. This shows that slant-F is a time dependent phenomenon, which peaked at early evening between 2100 and 2230 hr on this night.

The early evening slant-F echoes exhibit Doppler characteristics resembling that of the ground backscatter. The peak Doppler spectra of slant-F echoes, obtained by averaging over 5 range bins centered at 500 km, at 2130 hr are shown in Figure 8(a) for beams 3, 5, and 7. It is evident from this figure that the slant-F echoes exhibit very little spread about the peak Doppler frequency, similar to the Doppler characteristic of the ground backscatter. Unlike ground backscatter, however, the slant-F echoes exhibit shifts in the peak Doppler frequencies away from 0 Hz, with the amount of shifting depending on the azimuthal direction of the beam. The azimuthal dependence of peak Doppler frequency will be discussed in detail later in this section.

After 2200 hr, the slant-F echoes measured during the peak auroral activity period also exhibited shifts in the peak Doppler frequencies. This is evident in the ARD maps obtained at 2202 hr shown in Figure 6(c). In addition to the shift in the peak Doppler frequencies, the slant-F echoes at 2202 hr exhibited an increase in Doppler spread. This is evident in Figure 8(b), which displays the Doppler spectra of the slant-F echoes at 2130 and 2202 hr for the north-look beam. The increase in extent of the Doppler spread at 2202 hr suggests that the motion of the irregularities exhibits a much larger variance, which is in turn evidence of a disturbed ionosphere.

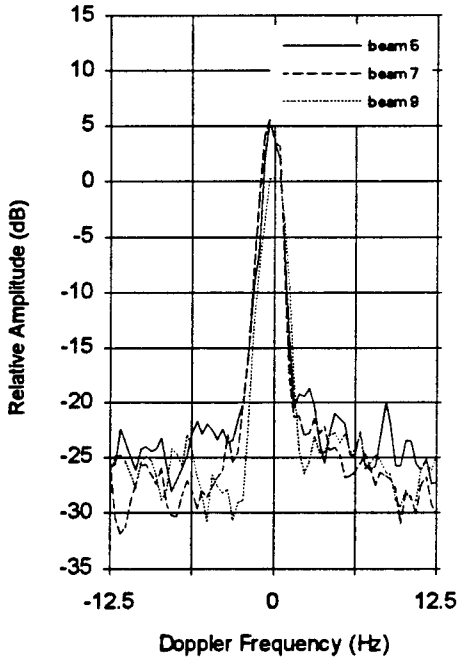

Figure 7. Doppler Spectra of Ground Backscatter at 2030 hr for Beams 5, 7, and 9.

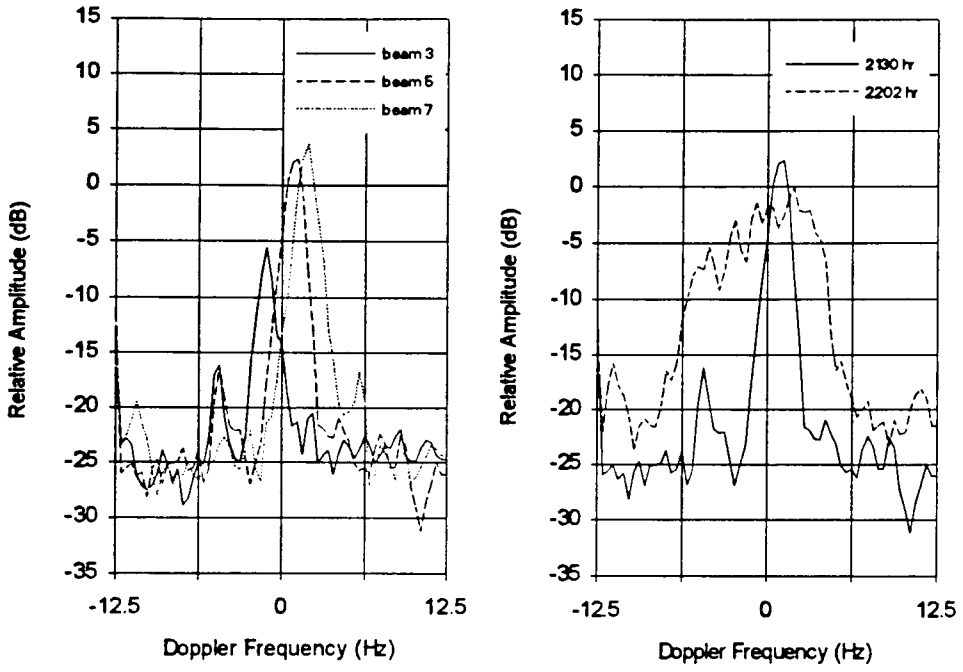

Figure 8. Doppler Spectra of Slant-F Echoes (a) at 2130 hr for Beams 3, 5, and 7, and (b) of Beam 5 at 2130 and 2202 hr.

3.1.4 CONSTANT-RANGE ECHOES

The constant-range backscatter was described in Section 3.1.1 as directly backscattered signals from the blobs of large-scale irregularities in the F-regions of sub-auroral and auroral ionosphere. The ionogram obtained at 2125 hr (Figure 4(b)) clearly exhibits two distinct leading edges of backscattered signals at 800 and 1300 km. The ARD maps at this time (Figure 6(b)) also show these backscattered signals with the leading edges at same slant range. The measurements at 2202 hr (Figure 6(c)) exhibit an increased number of echoes of distinct range and azimuthal extents. These backscattered signals appear in bands, extending approximately 150 km in slant range and 10 to 20 degrees in azimuth. The ARD maps obtained at 2242 hr show a significant decrease in the number of echoes, which is evidence of decrease in auroral activity. Therefore, the interval between 2100 and 2200 hr is characterized as having peak auroral activity.

The echoes due to the blobs of irregularities in the sub-auroral F-region (800 km) are characterized by both substantial shift in Doppler peaks and wider Doppler spreads. The intensities also increase during the peak auroral activity period. The peak Doppler spectra of the sub-auroral backscatter at 800 km slant range at 2130 hr is shown in Figure 9 for beams 5, 7, and 9. The shifts in peak Doppler

frequency and the extents of Doppler spread evident in this figure are greater than those for slant-F. The spreads are limited, however, suggesting that the longitudinal velocity variance is bounded.

In contrast to the sub-auroral echoes at 800 km, the auroral backscatter starting at 1250 km in Figure 6(b) and 1050 km in Figure 6(c) are characterized by intense and almost noise-like Doppler distributions. The peak Doppler frequency and spread cannot be inferred from these ARD maps. Figure 10(a) shows the Doppler spectra of the backscattered signal due to an irregularity at 1300 km (Figure 6(b)) for beams 5 and 7. The Doppler distribution of beam 5 exhibits wide frequency spread about a positive peak frequency, while the Doppler distribution of beam 7 exhibits similar spread about a negative peak frequency. The Doppler characteristic of beam 5 reveals that the irregularity structure is moving towards the radar with a large variance in velocity. However, the negative Doppler distribution of beam 7, which is 10 ° to the east with respect to beam 5, suggests that the same irregularity is moving away from the radar, which seems to be a contradiction. It will be shown in Section 3.2.2 that this is due to the limited Doppler bandwidth at a Waveform Repetition Frequency of 25 Hz.

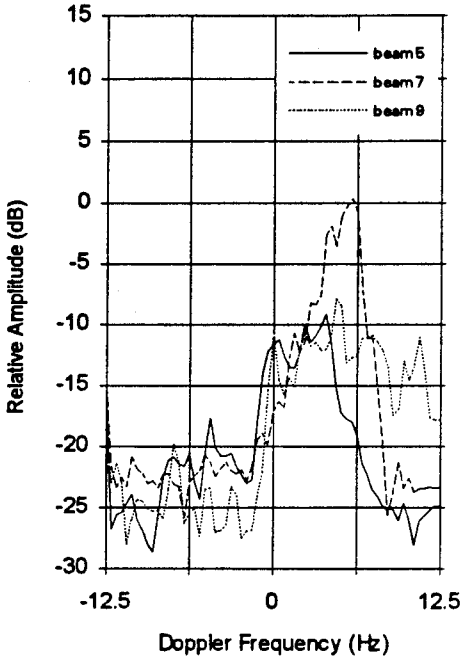

Figure 9. Doppler Spectra of Sub-Auroral Backscattered Signals at 2130 hr for Beams 5, 7, and 9.

Subsequently, during the peak auroral activity period, the Doppler spread of the auroral backscatter increased even further. Figure 10(b) displays the Doppler spectra of the auroral echoes observed at 1250 km at 2130 and 2202 hr for the north-look beam. The Doppler spectrum obtained at 2202 hr is not limited to the 25 Hz Doppler bandwidth and it resembles that of noise. This noise-like characteristic exhibited by the Doppler spectrum at 2202 hr is due to the high longitudinal velocity variance of the irregularities during the peak auroral activity period. Future data acquisition will use a higher WRF, thereby increasing the Doppler bandwidth. It will allow us to characterize the spread extent of the Doppler, and consequently, the velocity distribution of the auroral backscatter.

3.2 Discussion

In Section 3.1 we described the characteristics of ground backscatter and identified three types of backscattered signals from the high latitude ionosphere: slant-F, sub-auroral, and auroral backscatter. The three types have been distinguished by their origins in the ionosphere and their scattering mechanisms. Both the slant-F echoes and sub-auroral backscatter were described as the

backscattered signals from the sub-auroral F-region, while the auroral backscatter has been associated with the auroral F-region. The slant-F was defined as the backscattered signals due to the perpendicularity condition between the field-aligned, small-scale irregularities and the propagation vector of the signal. The constant range echoes were defined as the backscatter from the large-scale irregularities in the sub-auroral and auroral ionosphere. In this section, we discuss the ionospheric morphology underlying the data presented in Section 3.1.

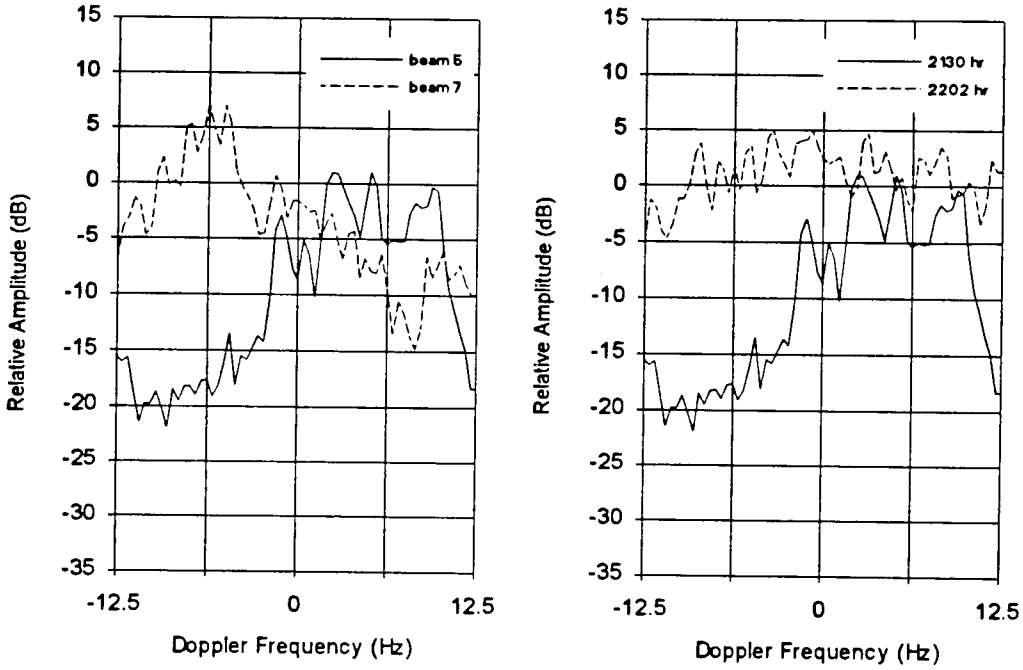

Figure 10. Doppler Spectra of the Backscattered Signal from the Auroral F-Region, (a) at 2130 hr for Beams 5 and 7 and (b) at 2130 and 2202 hr for Beam 5.

3.2.1 AZIMUTHAL DEPENDENCE OF PEAK DOPPLER FREQUENCY

In Section 3.1.3 the shifts in the peak Doppler frequencies of the slant-F echoes were shown to depend on azimuth. Figure 11 displays the peak Doppler frequencies as a function of the beam steering angle for the measurements at 2130 and 2202 hr. For the azimuths west of -5° (beam 4), the peak Doppler frequencies are negative, implying that the irregularities are moving away from the radar. The peak Doppler frequencies for the azimuths east of -5° are positive, implying that the irregularities are moving towards the radar. This suggests that the field-aligned irregularities in the sub-auroral F-region are moving east to west. Since the peak Doppler frequency is almost zero at

beam 4, the longitudinal velocity is near zero there. Therefore, the motion of the irregularities is transverse to the radar look direction at this azimuth beam.

It is interesting to note that the shift in peak Doppler frequency is not linear with respect to azimuth. This is probably because the longitudinal velocity measured by VALAR varies as the cosine of the aspect angle, where the aspect angle is defined as the angle between the radar steering vector and the velocity vector of the irregularities.

3.2.2 DOPPLER AMBIGUITY OF AURORAL BACKSCATTER

In Section 3.1.4 the characteristics of auroral backscatter were presented. The mean Doppler spectrum of the backscattered signals obtained at 2130 hr was presented in Figure 10. It was shown that the Doppler distribution of beam 5 exhibited frequency spread about a positive peak Doppler frequency, while beam 7 exhibited a similar spread about a negative peak Doppler frequency. The Doppler characteristic of beam 5 leads to a conclusion that the irregularity structure is moving towards the radar with a large velocity variance. However, the negative Doppler distribution of beam 7, which is 10° to the east with respect to beam 5, suggests that the same irregularity is moving away from the radar, which seems to be a contradiction.

This contradiction can be resolved as follows. A WRF of 25 Hz limits the Doppler bandwidth to -12.5 to 12.5 Hz, and consequently limits the maximum longitudinal velocity observable. The maximum unambiguous longitudinal velocity towards the radar for 25 Hz WRF and 10.58 MHz operating frequency is 177 m/sec. If the Doppler velocity is greater than 177 m/sec it will "wrap-around" and appear in the negative Doppler band. Considering the expected position of the auroral oval and the direction of the electrojet current relative to VALAR at 2130 hr, the Doppler shift should be positive. Furthermore, the longitudinal velocity component of the irregularity in beam 7 will be greater than in beam 5. Therefore, we can conclude that the negative Doppler observed in beam 7 is due to the aliasing of Doppler velocities greater than 177 m/sec toward the radar.

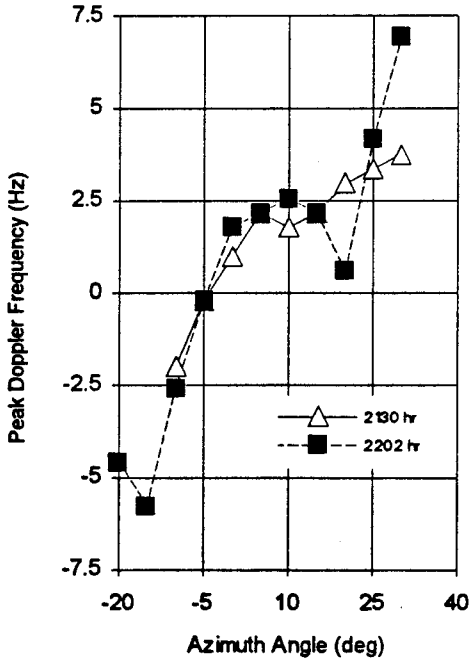

Figure 11. Peak Doppler Frequency of Slant-F Echoes with Respect to Azimuth Angle at 2130 and 2203 hr.

4. SUMMARY

HF auroral backscatter data collected using VALAR have been presented in this report. The capability of VALAR to observe auroral clutter and the availability of the elemental data make it a unique instrument for understanding and mitigating the problems associated with HF radars operating at or near high latitudes. The range-azimuth distribution and Doppler characteristics of HF auroral backscatter during a 2-hour period were presented. Slant-F echoes were identified as originating in the sub-auroral ionosphere, and exhibited small shifts in peak Doppler frequency and very small Doppler spread. The sub-auroral backscatter echoes were shown to exhibit greater shift and spread in Doppler in comparison to the slant-F echoes, but still confined within the 25 Hz Doppler bandwidth. The Doppler shifts and spreads of the echoes originating from the auroral ionosphere were shown to be much greater and not unambiguously resolved at a WRF of 25 Hz.

References

1. Moller, H.G. (1984), Backscatter results from Lindau. II. The movement of curtains of intense irregularities in the polar F layer, *J. Atmos. Terr. Phys.*, **36**:1487-1501.

2. Whalen, J. A. (1970), *Auroral Plotter and Nomograph for Determining Corrected Geomagnetic Local Time, Latitude for High Latitudes in the Northern Hemispheres*, AFCRL-70-0422, AD713170.

3. Gould, A. J. (1990), *A Thinned High Frequency Linear Antenna Array to Study Ionospheric Structure*, RADC-TR-90-186, Rome Air Development Center, Rome, NY, ADA240764.

4. Bates, H.F. (1960), Direct HF backscatter from the F region, *J. Geophys. Res.*, **65**:1993-2002.

5. Bates, H.F. (1971), The aspect sensitivity of spread-F irregularities, *J Atmos. Terr. Phys.*, **33**:111.

6. Elkins, T.J. (1980), *A Model for High Frequency Radar Auroral Clutter*, RADC-TR-80-122, Rome Air Development Center, Rome, NY, ADA091049.

7. Tsunoda, R. L., Basler, R. P., Showen, R. L., Walker, N. P., Frank, V. R., and Lomasney, J. M. (1981), *Investigation of High-Frequency Radar Auroral Clutter and Round-the-World Propagation*, Tech. Rep. 54, 66 pp., SRI Int., Menlo Park, Calif.

8. Vickery, J.F., Rino, C.L., and Potemra, T.A. (1980), Chatanika/TIAD observations of unstable ionization enhancements in the auroral F region, *Geophys. Res. Lett.*, **7**:789.

9. Montbriand, L. E. (1988), Auroral backscatter observed at HF from Ottawa, *Radio Sci.*, **23**:850-864.

MISSION

OF

ROME LABORATORY

Mission. The mission of Rome Laboratory is to advance the science and technologies of command, control, communications and intelligence and to transition them into systems to meet customer needs. To achieve this, Rome Lab:

a. Conducts vigorous research, development and test programs in all applicable technologies;

b. Transitions technology to current and future systems to improve operational capability, readiness, and supportability;

c. Provides a full range of technical support to Air Force Materiel Command product centers and other Air Force organizations;

d. Promotes transfer of technology to the private sector;

e. Maintains leading edge technological expertise in the areas of surveillance, communications, command and control, intelligence, reliability science, electro-magnetic technology, photonics, signal processing, and computational science.

The thrust areas of technical competence include: Surveillance, Communications, Command and Control, Intelligence, Signal Processing, Computer Science and Technology, Electromagnetic Technology, Photonics and Reliability Sciences.